

# Quantum Confinement in Hydrogen Bond

C. S. dos Santos\*, E. Drigo Filho,<sup>†</sup> R. M. Ricotta <sup>‡</sup>

June 27, 2021

## Abstract

In this work, the quantum confinement effect is proposed as the cause of the displacement of the vibrational spectrum of molecular groups that involve hydrogen bonds. In this approach the hydrogen bond imposes a space barrier to hydrogen and constrains its oscillatory motion. We studied the vibrational transitions through the Morse potential, for the NH and OH molecular groups inside macromolecules in situation of confinement (when hydrogen bonding is formed) and non-confinement (when there is no hydrogen bonding). The energies were obtained through the variational method with the trial wave functions obtained from Supersymmetric Quantum Mechanics (SQM) formalism. The results indicate that it is possible to distinguish the emission peaks related to the existence of the hydrogen bonds. These analytical results were satisfactorily compared with experimental results obtained from infrared spectroscopy.

---

\*Instituto de Biociências, Letras e Ciências Exatas, IBILCE-UNESP, São José do Rio Preto, SP, Brazil

<sup>†</sup>Instituto de Biociências, Letras e Ciências Exatas, IBILCE-UNESP, São José do Rio Preto, SP, Brazil

<sup>‡</sup>Faculdade de Tecnologia de São Paulo, FATEC/SP-CEETPS-UNESP, São Paulo, SP, Brazil

## INTRODUCTION

Hydrogen bond is an important interaction present in different systems in nature; the most famous examples of its occurrence are in water molecules and the DNA double helix,<sup>1</sup> and references therein. Particularly, biological macromolecules as proteins, nucleic acids and carboxylic acids have the molecular groups NH and OH in their structures. These groups induce the hydrogen bonds which are essential to stabilize the structures and play an important role in the behavior of these macromolecules. Several other systems like clathrates and liquid crystals present hydrogen bonds in their structures<sup>2</sup>.

Few years ago a modern definition of the hydrogen bond following a list of criteria was recommended, after a survey on recent results of the subject,<sup>3</sup>. According to this definition the hydrogen bond is an attractive interaction between a hydrogen atom from a molecule or a molecular fragment X-H in which X is more electronegative than H, and an atom or a group of atoms in the same or a different molecule, in which there is evidence of bond formation. The hydrogen bond can be classified as a donor-acceptor interaction. The notation of the bond is X-H $\cdots$ Y, where the dots represent the bond, X-H is the hydrogen bond donor and Y is the acceptor anion. The covalent bond is represented by X-H and the hydrogen bond is represented by H $\cdots$ Y. The high electro-negativity of atom X compared with the hydrogen atom in the X-H chemical bond makes the hydrogen to share part of its electronic density.

The different spectroscopy techniques, such as, Raman, infrared (IR), Terahertz (THz) and Nuclear Magnetic Resonance (NMR) spectroscopy, provide the identification of the vibrational transitions of the molecular groups involved, since they are sensitive to changes in the spectrum. Therefore, it is possible to know if a specific molecular group participate of the hydrogen bond, because the vibrational spectrum changes.

In this work it is proposed that quantum confinement effect is the main cause of delocalization of the vibrational spectrum of NH and OH groups when hydrogen bonds are formed.

Quantum confinement can be defined as the restricted space where the particles can move and it is generally introduced by a potential barrier created, for instance, due to electrostatic potentials, the presence of an interface between different materials or the presence

of a surface. The simplest case of confinement consists of a particle subject to an infinite square well potential treated in introductory quantum mechanics,<sup>4</sup>. In this confined regime, the motion of a particle is restricted to a well defined region of space and there is the appearance of discrete energy levels due to quantization effects. They appear once the size of the barrier is of the same magnitude as the de Broglie wavelength of the particle wave function. Confined systems have interesting applications; in material science the quantum confinement effect is well studied theoretically and experimentally in semiconductor physics, mainly in the study of quantum dots,<sup>5,6</sup>. If the size of the material is reduced, the electronic and optical properties are drastically changed and can be controlled; this is one of the main subjects of nanostructure science,<sup>7</sup>. There are other cases that may also be studied by confinement as, for instance, a system subjected to high pressure,<sup>8</sup>. Recent studies focus on theoretical as well as experimental investigations of hydrogen/halogen bonds in different confining environments,<sup>9 - 12</sup>.

In the approach used in this work the confinement is introduced by a potential barrier. In the formation of the hydrogen bond, the acceptor atom of the hydrogen bond introduces a barrier which prevents the free oscillation of the hydrogen atom attached to the donor atom. In this situation, the hydrogen is confined between two atoms and the energy levels are distorted by this confinement, i. e., there are vibrational frequency shifts. Vibrational frequency shifts can also be induced by high pressure,<sup>13 - 15</sup>.

Thus, the main interest of this paper is to study the hydrogen bonds present in biological macromolecules, particularly, to determine the vibrational transitions related to OH and NH groups. To overcome this proposal we used an analytical methodology based on the variational method associated to Supersymmetric Quantum Mechanics, (SQM).

The confined quantum mechanical problem is settled by considering the Schrödinger equation depending on a potential with a potential barrier. Considering that the hydrogen bonds are highly directional, the vibrations of the groups studied are better described by the one-dimensional Morse potential. If not by the potential barrier (without confinement) this potential presents exact analytical solution,<sup>16</sup>. However, by considering the confined case (with confinement) the problem is not exactly solvable and therefore an approximation method has to be introduced. At this point we use the formalism of SQM to calculate the

spectrum of wave functions and energies and use the variational method to treat the confined case, with a potential barrier. The transition energy between two adjacent states is calculated and the values obtained are compared with experimental spectroscopy data to validate the proposed hypothesis. The formalism of SQM coupled to the variational method has been a successful methodology to study many problems, in particular, the confined systems,<sup>6, 17-19</sup>.

Other theoretical models based on the use of the Morse potential have been proposed to describe high frequency and low frequency vibration modes of the hydrogen bonds,<sup>20-25</sup>. In the approach proposed here, unlike these models, there is no need either to use any coupling theory nor to enter new parameters in the Morse potential. The data used here refer only to the covalent bonding and to the length of the hydrogen bond, which reduces significantly the number of parameters.

## MODEL

A schematic model of a hydrogen bond between atoms X and Y is shown in Figure 1. In a hydrogen bonding, the hydrogen nuclei may oscillate within a region determined between a minimum distance ( $x_{min}$ ) and a maximum distance ( $x_{max}$ ). The value of  $x_{min}$  is given by the covalent radius ( $x_c$ ) of atom X and  $x_{max}$  is given by the length of the hydrogen bond ( $l_{x...y}$ ) subtracted by the van der Waals radius ( $x_{vw}$ ) of the acceptor atom, i.e.,

$$x_{max} = l_{X...Y} - x_{vw} \quad (1)$$

The origin of the coordinate system is located at the center of the atom X. Any distance used is computed from this point and it is considered center-to-center. The covalent radius is adopted by the condition of impenetrability of the hydrogen atom donor; the employment of the van der Waals radius is justified because it is a measure of the volume excluded by the acceptor atom, i.e., the hydrogen cannot penetrate this region. The atoms are considered as hard spheres and the hydrogen is treated as a material point, since the electron cloud is shared with the donor and the acceptor atoms.

As mentioned before, the vibrational energy of the system is described through the confined one-dimensional Morse potential. This potential has been widely used to describe oscillations of diatomic molecules,<sup>16-18</sup>. The energy absorbed/emitted is obtained from the

calculation of the energies of the ground state ( $n = 0$ ) (for NH and OH), the first excited state ( $n = 1$ ) (for NH and OH) and the second excited state ( $n = 2$ ) (only for OH). The energy of the absorbed/emitted photon is obtained from the difference between two adjacent levels. The energies of the confined case are evaluated by using the variational method associated to the formalism of SQM.

## SUPERSYMMETRIC QUANTUM MECHANICS, SQM

SQM is an algebraic method commonly used to exploit different aspects of non-relativistic quantum mechanical systems. It is particularly efficient to solve exactly all the quantum potential problems by means of the Hamiltonian factorization, thus providing the entire spectrum of wave functions with their respective energies together with a hierarchy of Hamiltonians, all related by the supersymmetric algebra,<sup>26</sup>. On the other hand, when the potential is non-exactly solvable, such as in a confined system, an approximation technique is needed and the variational method has already appeared as fully appropriate,<sup>16</sup>.

Thus, using the superalgebra a given Hamiltonian can be factorized in terms of bosonic operators. In  $\hbar = c = 1$  units, the Schrödinger equation can be rewritten as

$$H_1 = -\frac{d^2}{dx^2} + V_1(x) = A_1^+ A_1^- + E_0^{(1)} \quad (2)$$

where  $E_0^{(1)}$  is the lowest eigenvalue with ground state wave function satisfying

$$A_1^- \Psi_0^{(1)}(x) = 0 \quad (3)$$

and with the bosonic operators defined as

$$A_1^\pm = \left( \mp \frac{d}{dx} + w_1(x) \right) \quad (4)$$

where the superpotential  $w_1(x)$  satisfies the Riccati equation

$$w_1^2 - \frac{d}{dx} w_1 = V_1(x) - E_0^{(1)}. \quad (5)$$

and the ground state wave function has the following form

$$\Psi_0^{(1)}(x) = N \exp\left(-\int_0^x w_1(\bar{x}) d\bar{x}\right). \quad (6)$$

Thus a whole hierarchy of Hamiltonians can be constructed, with simple relations connecting the eigenvalues and eigenfunctions of the  $n$ -members,

$$H_n = A_n^+ A_n^- + E_0^{(n)} , \quad (7)$$

$$A_n^\pm = \left( \mp \frac{d}{dx} + w_n(x) \right) \quad (8)$$

$$\Psi_n^{(1)} = A_1^+ A_2^+ \dots \psi_0^{(n+1)} \quad E_n^{(1)} = E_0^{(n+1)}. \quad (9)$$

In equation (9), the upper index between parentheses refers to the hierarchy Hamiltonian member and the lower index to the level within the hierarchy.

## MATHEMATICAL FORMALISM

The one-dimensional Morse potential<sup>16</sup>, is given by

$$V_M = D_e (e^{-2\beta(x-x_{eq})} - 2e^{-\beta(x-x_{eq})}) \quad (10)$$

where  $D_e$  is the dissociation energy of molecule,  $\beta$  is the parameter related to the width of potential well and  $x_{eq}$  is the inter-nuclear equilibrium distance. The  $\beta$  parameter may be determined by treating the molecule as a frequency oscillator  $\nu$  and through experimental data. By expanding the Morse potential in a Taylor series around the equilibrium position to the second order we find that

$$\beta = \left( \frac{2\pi^2\mu}{D_e} \right)^{\frac{1}{2}} \nu . \quad (11)$$

The Schrödinger equation for a molecule subject to the Morse potential, according to the model, is written in one-dimensional Cartesian coordinates with the change of variables,  $y = \beta x$ . After multiplying both sides by  $\frac{2\mu}{\beta^2\hbar^2}$ , we obtain the Schrödinger equation

$$-\frac{d^2\Psi(y)}{dy^2} + \Lambda^2 (e^{-2(y-y_{eq})} - 2e^{-(y-y_{eq})}) \Psi(y) = \epsilon \Psi(y) \quad (12)$$

where

$$\Lambda^2 = \frac{2\mu D_e}{\beta^2 \hbar^2} \quad (13)$$

and

$$\epsilon = \frac{2\mu E}{\beta^2 \hbar^2} \quad (14)$$

where  $\mu$  is the reduced mass of the system. The Hamiltonian operator in equation (12) is given by

$$\hat{H}_M = -\frac{d^2}{dy^2} + \Lambda^2(e^{-2(y-y_{eq})} - 2e^{-(y-y_{eq})}) \quad (15)$$

Since the Schrödinger equation is exactly solvable, the process of factorization can be completely made and the whole hierarchy can be evaluated. The result is,<sup>16</sup>

$$\begin{aligned} V_{n+1}(y) &= \Lambda^2(e^{-2(y-y_{eq})} - 2e^{-(y-y_{eq})}) + 2n\Lambda e^{-(y-y_{eq})} \\ w_{n+1}(y) &= -\Lambda e^{-(y-y_{eq})} + \left(\lambda - \frac{2n+1}{2}\right) \\ \epsilon_0^{(n+1)} &= -\left(\Lambda - \frac{2n+1}{2}\right)^2. \end{aligned} \quad (16)$$

In addition we can calculate exactly the wave functions. The ground state wave function is evaluated by using equation (6) and is given by

$$\Psi_0^{(1)}(y) \propto \exp\left(-\Lambda e^{-(y-y_{eq})} - y\left(\Lambda - \frac{1}{2}\right)\right). \quad (17)$$

This wave function is then used to evaluate, through the SQM algebra, the wave function for the excited states by using equation (9); the first excited state is given by

$$\Psi_1^{(1)}(y) \propto -2\left(\Lambda e^{-(y-y_{eq})} - \Lambda + 1\right) \exp\left(-\Lambda e^{-(y-y_{eq})} - y\left(\Lambda - \frac{3}{2}\right)\right) \quad (18)$$

and the second excited state is given by

$$\begin{aligned} \Psi_2^{(1)}(y) &\propto (4\Lambda^2 e^{-2(y-y_{eq})} - 8\Lambda^2 e^{-2(y-y_{eq})} + 12\Lambda e^{-(y-y_{eq})} - \Lambda + 4\Lambda^2 - 14\Lambda + 12) . \quad (19) \\ &\quad \exp\left(-\Lambda e^{-(y-y_{eq})} - y\left(\Lambda - \frac{5}{2}\right)\right) . \end{aligned}$$

The wave functions given in (17), (18) and (19) are obtained to the exact system, non-confined or with no hydrogen bond. We refer to them as  $\Psi_{n(\text{non-confined})}$ . For the confined system a potential barrier is introduced meaning that the wave functions must be zero outside the barrier. As the system is no longer exact, it is necessary to use an approximative method, which we choose to be the variational method. Thus, based on previous results,<sup>6</sup>

and<sup>17</sup>, the eigenfunctions are multiplied by the term  $(y_{max} - y)(y - y_{min})$ , i.e., the wave functions become zero at the edges of the confinement region. For the ground state, this approach is equivalent to introduce two additional terms in the superpotential  $w_1$ , which corresponds to an infinite barrier in the confinement border,  $V_1(y_{max}) = V_1(y_{min}) = \infty$ .

Adopting this procedure, the wave functions are defined for the region of space in which we are interested and, consequently, the probability of finding the hydrogen outside the confinement region must be zero. Thus, the trial wave functions to be used in the variational method are given by

$$\Psi_n^{(1)}(confined) \propto \Psi_n^{(1)}(non-confined) \cdot (y_{max} - y)(y - y_{min}) \quad (20)$$

and we will only need the cases of  $n = 0, 1, 2$ .

The energies for the confined case are obtained by solving

$$E_n = \frac{\int_{y_{min}}^{y_{max}} \Psi_n^* \hat{H}_M \Psi_n dy}{\int_{y_{min}}^{y_{max}} \Psi_n^* \Psi_n dy} \quad (21)$$

where  $\hat{H}_M$  is the Hamiltonian of the system given by equation (15) and  $\Psi_n$  are the trial wave functions given by equation (20), where  $\Psi_n^{(non-confined)}$  are given by (17), (18) and (19). The integration limits are the covalent radius of the atom for which the hydrogen is chemically bound ( $x_{min}$ ) and the van der Waals radius complementary of hydrogen bond ( $x_{max}$ ). The results of energy are presented in  $cm^{-1}$  units (inverse wavelength) to facilitate comparison with the spectroscopic results.

## RESULTS

The hydrogen bonds studied involve the NH and OH groups. Tables 1 and 2 below list the necessary parameters, obtained experimentally,<sup>27-29</sup>.

**Table 1.** Parameters used in the NH and OH groups energy evaluations,<sup>27</sup>.

	<i>NH</i>	<i>OH</i>
Equilibrium distance ( $x_{eq}$ )	1.0362 Å	0.9697 Å
Harmonic vibrational wavenumber ( $\omega$ )	$3282cm^{-1}$	$3738cm^{-1}$
Energy dissociation ( $D_e$ )	3.47 eV	4.39 eV
Reduced mass ( $\mu$ )	$1.5614.10^{-27}kg$	$1.5746.10^{-27}kg$

**Table 2.** Covalent and van der Waals radius used for the nitrogen and oxygen atoms,<sup>28, 29</sup>.

	<i>N</i>	<i>O</i>
Covalent radius ( $x_c$ )	0.71 Å	0.66 Å
van der Waals radius ( $x_{vw}$ )	1.55 Å	1.52 Å

## Results for NH group

### Non-confined case

The  $\beta$  parameter in Morse potential is determined using the values given in Table 1 through the relation (11) and for NH group it is given by  $2.3168.10^{10}m^{-1}$ . The value of the constant  $\Lambda$  for NH group, given by equation (13), is 17.0534.

In the situation free of any confinement, the calculation of the transition from the first excited state to the ground state is made according to equation (16). In this case, in spectroscopic units, this value corresponds to  $\Delta E_{1 \rightarrow 0} = E_1 - E_0 = 3089cm^{-1}$  and it should be checked by means of spectroscopy. By IR spectroscopy with polypeptides, an absorption band in  $3090cm^{-1}$  is observed and it has been described as a vibration frequency of the NH molecular group,<sup>30</sup>. This value is very close to the calculated and can be identified, according to the proposed model, as vibration of NH without formation of hydrogen bonding.

## Confined case

When the NH group form molecular hydrogen bonding, the vibration frequency is shifted. An interesting system where this effect can be observed is in proteins. These may be in the form of  $\alpha$ -helix,  $\beta$ -sheet or random. In this helicoidal format the hydrogen bonding is between the amine group of an amino acid and the oxygen of the carboxyl group of another amino acid. Thus, proteins consist in a good system to verify the quantum confinement effect in hydrogen bonding. It is found in the literature that proteins in  $\alpha$ -helix format present hydrogen bond lengths around  $2.80\text{\AA}$ ,<sup>31</sup>. Considering the uncertainty of experimental results, the values of  $2.75\text{\AA}$ ,  $2.80\text{\AA}$  and  $2.85\text{\AA}$  were used as the maximum distance of the hydrogen oscillation, according to the equation (1). Solving equation (21) numerically, the results for the emission/absorption for proteins in  $\alpha$ -helix are indicated below in Table 3.

**Table 3.** Energy levels of proteins with hydrogen bonding, for different values of  $x_{max}$  in ( $cm^{-1}$ ) units.

$x_{max}$	$E_0$	$E_1$	$\Delta E_{1 \rightarrow 0}$
$2.75\text{\AA}$	-26105	-22643	3461
$2.80\text{\AA}$	-26245	-22835	3410
$2.85\text{\AA}$	-26306	-23010	3296

The hemoglobin, a metalloprotein present in the red blood cells of all vertebrates, is constituted of four  $\alpha$ -helix chains. IR spectroscopy realized to verify the alterations caused by  $\beta$ -thalassemia disorder, a reduction or absence synthesis of the beta chains of hemoglobin,<sup>32</sup>, showed peaks around  $3050cm^{-1}$  and  $3290cm^{-1}$ , that can be identified as vibrations of the NH group in the situations free of confinement and confined, or with or without hydrogen bond, respectively. By considering  $2.85\text{\AA}$  as the maximum distance of the hydrogen oscillation, the comparison of our theoretical result for the confined case ( $3296cm^{-1}$ ) with these results shows an error of 0.18%. Thus we expect that other proteins in  $\alpha$ -helix format present absorption peaks around  $3296cm^{-1}$ . In fact, other proteins in the  $\alpha$ -helix format present transitions verified by IR spectroscopy that corroborate with our results, as shown below.

Keratin, for instance, is a protein found in abundance in life, in the human epidermis, hair,

nails, feathers, porcupine quills, etc. IR spectroscopy of virgin human hair (i.e., no chemical intervention) and horse hair, using lithium bromide and hydrochloric acid as reagent,<sup>33</sup>, showed the keratin absorption bands of hair with and without cuticle. Similar studies were carried out with a dried sample of goose feather followed by a soaked sample using heavy water,<sup>34</sup>. The IR spectroscopy studies with some peptides, polyamides and fibrous proteins used swan feather wing and horse hair as a source of keratin,<sup>35</sup>.

Other protein having  $\alpha$ -helix structure is rhodopsin, which can be found in the eye retina. IR spectroscopy with bovine rhodopsin Langmuir-Blodgett films,<sup>36</sup>, showed an absorption peak in  $3295\text{cm}^{-1}$ ; the theoretical result presents 0.03% error relative to this experimental result.

The sodium-potassium pump (Na<sup>+</sup>/K<sup>+</sup>-ATPase) present in cells is another protein which contains several  $\alpha$ -helices,<sup>37</sup>. The IR spectroscopy carried out in an aqueous medium of three different ionic compositions presented absorption peaks; in all types of solvent there is a peak located in  $3285\text{cm}^{-1}$ ; the theoretical result presents 0.33% error relative to this experimental result.

Table 4 summarizes the results discussed above.

**Table 4.** Results for absorption/emission values  $\Delta E_{1 \rightarrow 0} = E_1 - E_0$ , in ( $\text{cm}^{-1}$ ) units for the non-confined and confined cases with deviations relative to the experimental result.

	Non-Confined (no hydrogen bond)	Confined (with hydrogen bond)	Deviation from experimental
Theoretical	3089	3296	
Hemoglobin with $\beta$ -thalassemia disorder, <sup>32</sup>	3050	3290	0.18
Normal Hair, <sup>33</sup>	3066	3300	0.12
Hair without cuticle, <sup>33</sup>	3062	3295	0.03
Horse Hair, <sup>33</sup>	-	3293	0.09
Goose feather, <sup>34</sup>	3100	3300	0.12
Swan Feather Wing, <sup>35</sup>	3070	3290	0.18
Horse Hair, <sup>35</sup>	3080	3295	0.03
Rhodopsin (Retina eye), <sup>36</sup>	-	3295	0.03
Sodium-Potassium Pump, <sup>37</sup>	-	3285	0.33

## Results for OH group

### Non-confined case

In the case of OH group, the transition from the second to the first excited state ( $\Delta E_{2 \rightarrow 1} = E_2 - E_1$ ) is also studied. According to the formalism described, the  $\beta$  parameter, equation (11), for the OH group is  $2.3558 \cdot 10^{10} m^{-1}$  and the  $\Lambda$  constant value is 18.9424. In the situation free of any type of confinement, i.e. with no hydrogen bond, the transitions between adjacent states were evaluated by using equation (16); the results are shown in Table 5.

**Table 5.** Eigenvalues of energy to OH obtained by the model described in  $cm^{-1}$  units.

$E_0$	$E_1$	$E_2$	$\Delta E_{1 \rightarrow 0}$	$\Delta E_{2 \rightarrow 1}$
-33560	-30019	-26676	3541	3343

## Confined case

Carboxylic acid dimers are held by hydrogen bonds between the hydroxyl. By means of neutron diffraction, differently to the X-ray diffraction, one can obtain the distances between the hydrogen atom and the other atoms that compose the network,<sup>2</sup>. Figure 2 shows the distance between the hydrogen, linked to the donor atom, and the acceptor atom of the bond. Thus, to find the maximum distance of oscillation is necessary to sum the equilibrium distance of the OH bond to the length of hydrogen bond, i. e., the maximum distance is given by

$$x_{max} = x_{eq} + l_{H-O} - x_{vw} . \quad (22)$$

Three types of carboxylic acids in the form of dimers, are studied in this work, the lengths of the hydrogen bonds are reported in Table 6.

**Table 6.** Length of hydrogen bonds in dimers of different acids,<sup>2</sup>.

	Trifluoroacetic acid	Acetic acid	Formic acid
Bond length ( $l_{H-O}$ )	1.658 Å	1.642 Å	1.660 Å

Using the values of Table 6 to find the maximum distance of oscillation of hydrogen according to the equation (22) and solving equation (21) with wave functions given by (20) and (17)-(19) we find the value of emission/absorption energies for carboxylic acid dimers, shown in Table 7.

**Table 7.** Energy levels of different systems, in ( $cm^{-1}$ ) units.

	$E_0$	$E_1$	$E_2$	$\Delta E_{1 \rightarrow 0}$	$\Delta E_{2 \rightarrow 1}$
Trifluoroacetic acid	-32953	-29282	-26270	3671	2944
Acetic acid	-32767	-29342	-26270	3425	3072
Formic acid	-32973	-29277	-26342	3696	2935

The trifluoroacetic acid was analyzed in neon and argon matrices, in its monomeric form, in cyclic dimers and also in the deuterated form ( $CF_3COOD$ ) by means of IR spec-

troscopy,<sup>38</sup>. In neon matrix the dimer of trifluoroacetic acid presented emission/absorption of  $2922\text{cm}^{-1}$ , described as the vibration of the OH molecular group, because when the acid is deuterated this peak disappears. The theoretical value presents 0.75% of error relative to this experimental value, considering the transition between the second excited state and the first excited state,  $\Delta E_{2\rightarrow 1} = E_2 - E_1$ .

Acetic acid was also analyzed by IR spectroscopy,<sup>39</sup>. There were treated several dimers of carboxylic acids. The values of  $3067\text{cm}^{-1}$  in gas phase,  $3100\text{cm}^{-1}$  carbon tetrachloride solution ( $CCl_4$ ) and  $3080\text{cm}^{-1}$  in liquid phase agree with a transition  $\Delta E_{2\rightarrow 1}$  (Table 7) of the confined case, with theoretical errors smaller than 0.9%, obtained for the case where the acid was in  $CCl_4$  solution.

IR spectroscopy was also used to analyse the formic acid photocatalytic decomposition process,<sup>40</sup>. When it is analyzed on the catalyst surface of  $TiO_2$ , without any additive, an absorption peak near  $3698\text{cm}^{-1}$  can be noted, compatible to the transition  $\Delta E_{1\rightarrow 0}$  (Table 7). This peak is attributed by the authors to the OH group, which during the reaction is displaced to values below  $3668\text{cm}^{-1}$ . This can be explained by the dissociation of the OH group during decomposition, preventing the formation of hydrogen bond and weakening the bonds still existing.

The IF spectroscopy of photocatalytic decomposition of formic acid was analyzed in<sup>41</sup>, showing transitions identified as the vibration of the OH group, which agrees with the transition of  $\Delta E_{1\rightarrow 0}$  (Table 7). Table 8 summarizes the results discussed above.

**Table 8.** Results for absorption/emission values  $\Delta E_{1\rightarrow 0} = E_1 - E_0$ , in ( $\text{cm}^{-1}$ ) units for the non-confined and confined cases with deviations relative to the experimental result.

	$\Delta E_{1 \rightarrow 0}$	$\Delta E_{2 \rightarrow 1}$	Deviation from experimental (%)
Trifluoroacetic acid, <sup>38</sup>	-	2922	0.75
Theoretical	3671	2944	
Acetic acid, <sup>39</sup>			
Gas phase	-	3067	0.16
In $CCl_4$ solution	-	3100	0.90
Liquid phase	-	3080	0.26
Theoretical	3425	3072	
Formic acid, <sup>40</sup>	3698	-	0.05
Formic acid, <sup>41</sup>	3697	-	0.03
Theoretical	3696	2935	

## CONCLUSIONS

In this work the quantum confinement effect in hydrogen bonds explains the shift in the emission spectrum of NH and OH groups. In all the cases mentioned the distortion in the spectrum when the bond is formed is considerable and measurable, and is easily distinguished from the non-confined case, with no hydrogen bond. This shift occurs because the hydrogen bond imposes a barrier to the hydrogen and prevents it from having freedom in its oscillatory motion.

Quantitative results obtained for the vibrational transitions of the groups mentioned agree with the experimental results reported in the literature, reenforcing the applicability of the proposal and the reliability of this quantum mechanical methodology. The errors between the theoretical values entered by the variational method and the experimental data analyzed are small, the largest percentage error obtained in the calculations is smaller than 1.0%.

The test wave functions used in the confined case, obtained with the aid of the SQM formalism, are appropriate to describe the phenomenon. As a final result of the construction of these wave functions, the polynomial terms are multiplied by the wave functions of the free

system, with no confinement. This term of confinement is sufficient to obtain the numerical results presented.

As a final remark, the treatment proposed here can be extended to the study of other molecular groups, as FH and CH, involved in hydrogen bonds.

## References

1. E. Arunan, G. R. Desiraju, R. A. Klein, J. Sadlej, S. Scheiner, I. Alkorta, D. C. Clary, R. H. Crabtree, J. J. Dannenberg, P. Hobza, H. G. Kjaergaard, A. C. Legon, B. Mennucci, and D. J. Nesbitt, *Pure Appl. Chem.*, **2011**, 83, 16191636
2. G. A. Jeffrey, *An Introduction to Hydrogen Bonding*, Ed. Oxford University Press, New York, **1997**
3. E. Arunan, G. R. Desiraju, R. A. Klein, J. Sadlej, S. Scheiner, I. Alkorta, D. C. Clary, R. H. Crabtree, J. J. Dannenberg, P. Hobza, H. G. Kjaergaard, A. C. Legon, B. Mennucci, and D. J. Nesbitt, *Pure Appl. Chem.*, **2011**, 83, 16371641
4. D. J. Griffiths, *Introduction to Quantum Mechanics*, Ed. Pearson Pearson Prentice Hall, 2nd Edn., **2004**
5. S. Y. Ren, *Solid State Communications*, **1997**, 102, 479-484
6. E. Drigo Filho and R. M. Ricotta, *Phys. Lett. A*, **2002**, 299, 137
7. P. Harrison, *Quantum wells, wires and dots*, Ed. John Wiley and Sons, **2005**
8. A. Kangarlu, H. R. Chandrasekhar, M. Chandrasekhar and Y. M. Kapoor, F. A. Chambers, B. A. Vojak, J. M. Meese, *Phys. Rev. B*, **1988**, 38, 9790-9796
9. P. Lipkowski, J. Kozłowska, A. Roztoczyńska and W. Bartkowiak, *Phys. Chem. Chem. Phys.*, **2014**, 16, 1430-1440
10. A. Roztoczyńska, J. Kozłowska, P. Lipkowski, W. Bartkowiak, *Chem. Phys. Lett.*, **2014**, 608, 264-268
11. M. G. Sarwar, D. Ajami, G. Theodorakopoulos, I. D. Petsalakis, and J. Rebek Jr., *J. Am. Chem. Soc.*, **2013**, 135, 13672-13675
12. D. Ajami, H. Dube and J. Rebek Jr., *J. Am. Chem. Soc.*, **2011**, 133, 9689-9691
13. R. R. Wiederkehr and H. G. Drickamer, *J. Chem. Phys.*, **1958**, 28, 311-315

14. M.R. Zakin, D.R. Herschbach, *J. Chem. Phys.*, **1986**, 85, 23762383
15. M. R. Zakin, ;D. R. Herschbach, *J. Chem. Phys.*, **1988**, 89, 2380-2387
16. E. Drigo Filho and R. M. Ricotta, *Phys. Lett A*, **2000**, 296, 296-276
17. F. R. Silva and E. Drigo Filho, *Chem. Phys. Lett.*, **2010**, 498, 198-202
18. E. Ley-Koo, S. Mateos-Cortés and G. Villa-Torres, *Intern. J. Quantum Chem. Phys.*, **1998**, 58, 23-28
19. Y. P. Varshni, *Mod. Phys. Lett. A*, **2004**, 19, 2757-2764
20. L. Leviel and Y. Marechal, *J. Chem. Phys.*, **1971**, 54, 1104-1107
21. N. Rekik N, B. Oujia and M. J. Wójcik, *J. Chem. Phys.*, **2008**, 352, 65-76
22. I. Noureddine, G. Houcine and O. Brahim, *Intern. J. Quantum Chem.*, **2012**, 112, 1006-1015
23. G. Houcine, I. Noureddine and O. Brahim, *Intern. J. Quantum Chem.*, **2012**, 112, 1373-1383
24. Y. Marechal and A. Witkowski, *J. Chem. Phys.*, **1968**, 48, 3697-3705
25. P. Blaise, M. J. Wójcik and O. H. Rousseau, *J Chem. Phys.*, **2005**, 122, 64306
26. C. V. Sukumar, *J. Phys. A: Math. Gen.*, **1985**, 18 L57
27. R. Janoschek, *Pure and Appl. Chem.*, **2001**, 73, 1521-1553
28. B. Cordero, V. Gómez, A. E. Platero-Prats, M. Revés, J. Echeverría, E. Cremades, F. Barragán and S. Alvarez, *Dalton Transactions*, **2008**, 2832-2838
29. A. Bondi, *J. Phys. Chem.*, **1964**, 68, 441-451
30. R. M. Badger and H. Rubalcava, *Proc. Nat. Acad. Sci.*, **1954**, 40, 12-17
31. D. Voet and J. G. Voet, *Biochemistry*, Ed. Wiley, **1995**, 2nd Edn, New York

32. K. Z. Liu K Z, K. S. Tsang, C. K. Li, R. A. Shaw, H. H. Mantsch, *Clin. Chem.*, **2003**, 49, 1125-1132

33. C. B. Baddiel, *J. Mol. Biol.*, **1968**, 38, 181-199

34. K. D. Parker, *Biochim. Biophys. Acta*, **1955**, 17, 148-149

35. E. M. Bradbury and A. Elliot., *Polymer*, **1963**, 4, 47-59

36. I. M. Pepe, M. K. Ram, S. Paddeu and C. Nicolini, *Thin Solid Films*, **1998**, 327-329, 118-122

37. U. P. Fringeli, H-J. Apell, M. Fringeli and P. Lauger, *Biochim. Biophys. Acta*, **1989**, 984, 301-312

38. L. Redington and K. C. Lin, *Spectrochim. Acta A*, **1971**, 27, 2445-2460

39. S. Bratoz, D. Hadzi and N. Sheppard, *Spectrochim. Acta*, **1956**, 8, 249-261

40. J. Araña, C. Garriga i Cabo, J. M. Dona-Rodriguez, O. González-Díaz, J. A. Herrera-Melian, J. Pérez-Peña, *App. Surf. Sci.*, **2004**, 239, 60-71

41. T. Chen, G. Wu, Z. Feng, G. Hu, W. Su, P. Ying and C. Li, *Chin. J. Catal.*, **2008**, 29, 105-107

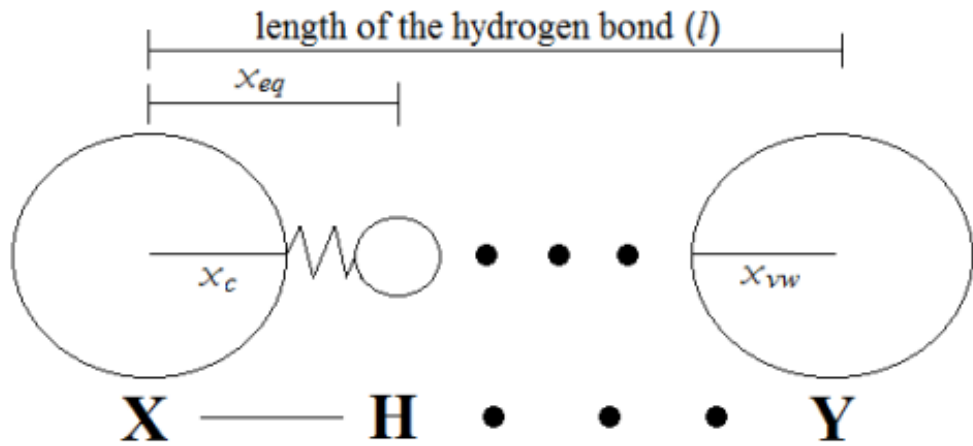


Figure 1: Schematic one-dimensional model, where  $x_c$  is the covalent radius of the donor atom X,  $x_{vw}$  is the van der Waals radius of the acceptor atom Y and  $x_{eq}$  is the equilibrium distance of covalent bond.

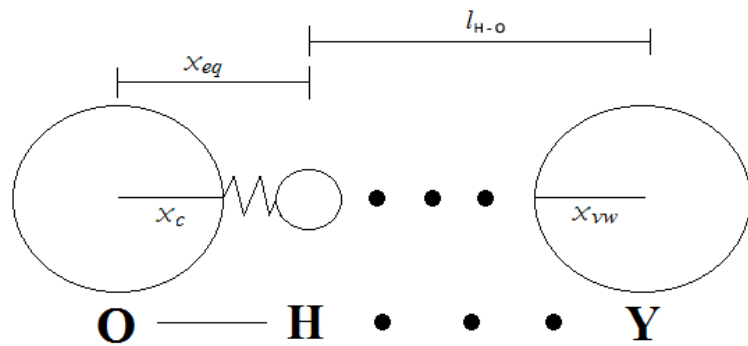


Figure 2: Schematic one-dimensional model for hydrogen bond for the group OH, remarking the length of hydrogen bond,<sup>2</sup>.